



Research

Current and future land fire risk mapping in the southern region of Sumatra, Indonesia, using CMIP6 data and GIS analysis



Muhammad Rendana¹ · Wan Mohd Razi Idris² · Sahibin Abdul Rahim³ · Hazem Ghassan Abdo⁴  · Hussein Almohamad⁵ · Ahmed Abdullah Al Dughairi⁵ · Jasem A. Albanai⁶

Received: 23 April 2023 / Accepted: 3 July 2023

Published online: 15 July 2023

© The Author(s) 2023 [OPEN](#)

Abstract

Land fires lead to a deterioration of environmental quality and have perilous social and economic aspects. One method for mitigating this hazard is to determine the range of fire risk areas. Thus, this study aimed to analyze the current and potential future fire risk in the Ogan Komering Ilir, southern Sumatra region of Indonesia, using CMIP6 data and geospatial technology. In order to analyze fire risk areas, the Landsat 8 satellite image from 2021 (as a baseline period) was used. Variables like the normalized difference moisture index (NDMI), the normalized difference vegetation index (NDVI), and the land surface temperature (LST) were extracted from the satellite image. Then, the standard precipitation index (SPI) was determined using rainfall data from meteorological stations. For future period prediction (periods 2021–2040 and 2041–2060), this study used future climate data from the CMIP6. By overlaying these variables, current and future fire risk zone maps were produced. The results obtained showed that in the current period, around 726.4 km² (4.2%) of the area was at high fire risk, then 5,621.3 km² (32.7%) and 10,835.3 km² (63.1%) were at moderate and low fire risk zones, respectively. Furthermore, for the future period, this study estimated there was an increase in high fire risk areas of about 14% during 2021–2040 and 30% during 2041–2060. This was recorded in the southern and northern parts of the study area. Fire risk areas were strongly associated with NDMI, NDVI, and LST. The study's findings may be useful for land fire management in fire-prone areas.

Article Highlights

- Future map scenario reveals up to an increase of forest fire in South Sumatra.
- CMIP6 and GIS together performed best in mapping forest fire.
- Forest fire events are closely associated with the NDMI, NDVI and LST.

Keywords Environment · CMIP6 · Fire risk mapping · Landsat 8 · Land surface temperature

✉ Hazem Ghassan Abdo, hazemabdo@tartous-univ.edu.sy | ¹Department of Chemical Engineering, Faculty of Engineering, Universitas Sriwijaya, Indralaya, Sumatra Selatan 30662, Indonesia. ²Department of Earth Sciences and Environment, Faculty of Science and Technology, Universiti Kebangsaan Malaysia, 43600 Bangi, Selangor, Malaysia. ³Department of Environmental Science, Faculty of Science and Natural Resources, Universiti Malaysia Sabah, 88400 Kota Kinabalu, Sabah, Malaysia. ⁴Geography Department, Faculty of Arts and Humanities, Tartous University, Tartous, Syria. ⁵Department of Geography, College of Arabic Language and Social Studies, Qassim University, Buraydah 51452, Saudi Arabia. ⁶Marine Monitoring Section, Water Quality Monitoring Department, Environmental Public Authority, Salmia, Kuwait.



SN Applied Sciences

(2023) 5:210

| <https://doi.org/10.1007/s42452-023-05432-6>

1 Introduction

Forests are one of the most prominent natural resources for maintaining the stability and sustainability of an ecosystem [1, 2]. Forest fires are the most prominent and widespread threat to global forests [3–5]. The forest fire can deteriorate ecosystem function and threaten the species that live within them [6, 7]. Based on the 2019 authority report, around 135,000 ha of Indonesian forests have been degraded by fire. One of the largest forest fire cases in Indonesian provinces comes from the South Sumatra region. This region is prone to forest fires because the majority of areas are covered with peatland. The land use conversion for the agricultural purpose is the main contributor for peatland fire in this region [8]. In 2019, the total burned area in South Sumatra reached 52,716 ha.

In this region, the majority of fire cases come from the Ogan Komering Ilir regency. Every year, especially during the dry season, many lands are burned, leading to a severe smoke hazard in the Southeast Asian region [9]. Some necessary actions have been carried out by authorities to control fire using conventional methods by humans and also the advanced technique using water bombing from the air [10]. However, methods to suppress or control fire activity are still being discovered at this time. Many researchers believe that creating a land fire risk map can help identify hotspots before they become a fire [11, 12]. This fire risk evaluation before this crisis time was important for fire control in the forest area and became a guide for land fire management.

Several studies have successfully applied remote sensing and geospatial technology for fire risk studies [13, 14]. Remote sensing and GIS are preferred because they are available with rapid and simple access, broad visibility, and low time and cost consumption [15]. For instance, Sakellariou et al. [16] used a remote sensing technique based on the normalized difference moisture index (NDMI) to identify high fire hazards on a small Greek island. Liu et al. [17] discovered a strong relationship between surface temperature and fire risk areas. Glushkov et al. [18] used the Sentinel satellite data to analyze land fire risk in Russia, while Achour et al. [19] used the Landsat data to monitor fire risk in Tunisia. The outputs of both studies exhibited a satisfactory result in detecting fire risks.

The impact of El Niño-Southern Oscillation (ENSO) and Indian Ocean Dipole (IOD) on forest fire events has been extensively discussed for forests in the tropical and subtropical regions. The combination of La Nina (cold ENSO) and IOD was obtained to be associated with anomalous high fire occasions in the forests of Northwest China

[20]. Meanwhile, El Niño (warm ENSO) and IOD have resulted to an increase in forest fire frequency in North-western Brazil [21], Australia and other tropical regions [22, 23]. A previous study by Nurdiani et al. [24] revealed the influence of La Nina increased the monthly rainfall in Indonesia and caused the dry season shorter. Thus, this circumstance would make the association between rainfall and burned areas reduced. But, we assumed that the effect of La Nina and IOD on tropical peatland forest fire especially in Southern land of Sumatra is still vague. Also, the link of La Nina occasions with high fire risk of Sumatran forests has not been examined.

Section 1 consists a brief introduction, and Sect. 2, materials and methods, that includes 4 subsections such as study area, data sources, preparation of associated-variables for land fire risk, and current and future land fire risk analysis. Section 3 consists the results and discussion, and Sect. 4 presents the conclusion. According to the above studies, there are limited studies that evaluate the fire risk in the future using a forecast climate model. CMIP6 data has offered a new strategy for facing the climate change issue. It can be used and combined with satellite image analysis to obtain the location of fire-prone zones within the forest region in the future. Therefore, the objective of this study aims to analyze the current and potential future forest fire risk zones in Ogan Komering Ilir, southern Sumatra, Indonesia using CMIP6 and GIS. The output of this study is useful for the authority in arranging an effective policy to mitigate a severe forest fire event in that region.

2 Materials and methods

2.1 Study area

The Ogan Komering Ilir (OKI) regency is situated in the southern part of Sumatra island (Fig. 1). The total area of this region is around 19,023 km². The OKI is situated between longitudes 104°40'00"E and 106°40'00"E and latitudes 2°40'00"S and 4°0'00"S. The OKI is administratively included in the South Sumatra Province of Indonesia. This region often experiences fire events almost in every year. Since the forest type of the study area is peat swamp forest, the fires makes the changes of peat soil properties, and diminishes vegetations cover and their composition. Then, the drought effect may rise the plant degradation and release carbon dioxide to atmosphere [25]. The fires have disturbed the endangered species in this region such as *Panthera tigris sumatrae* and *Elephas maximus sumatranus*. The tigers and elephants was often found in the villages due to habitat fragmentation thus this situation triggers the human-animal conflict. For instance, the fires

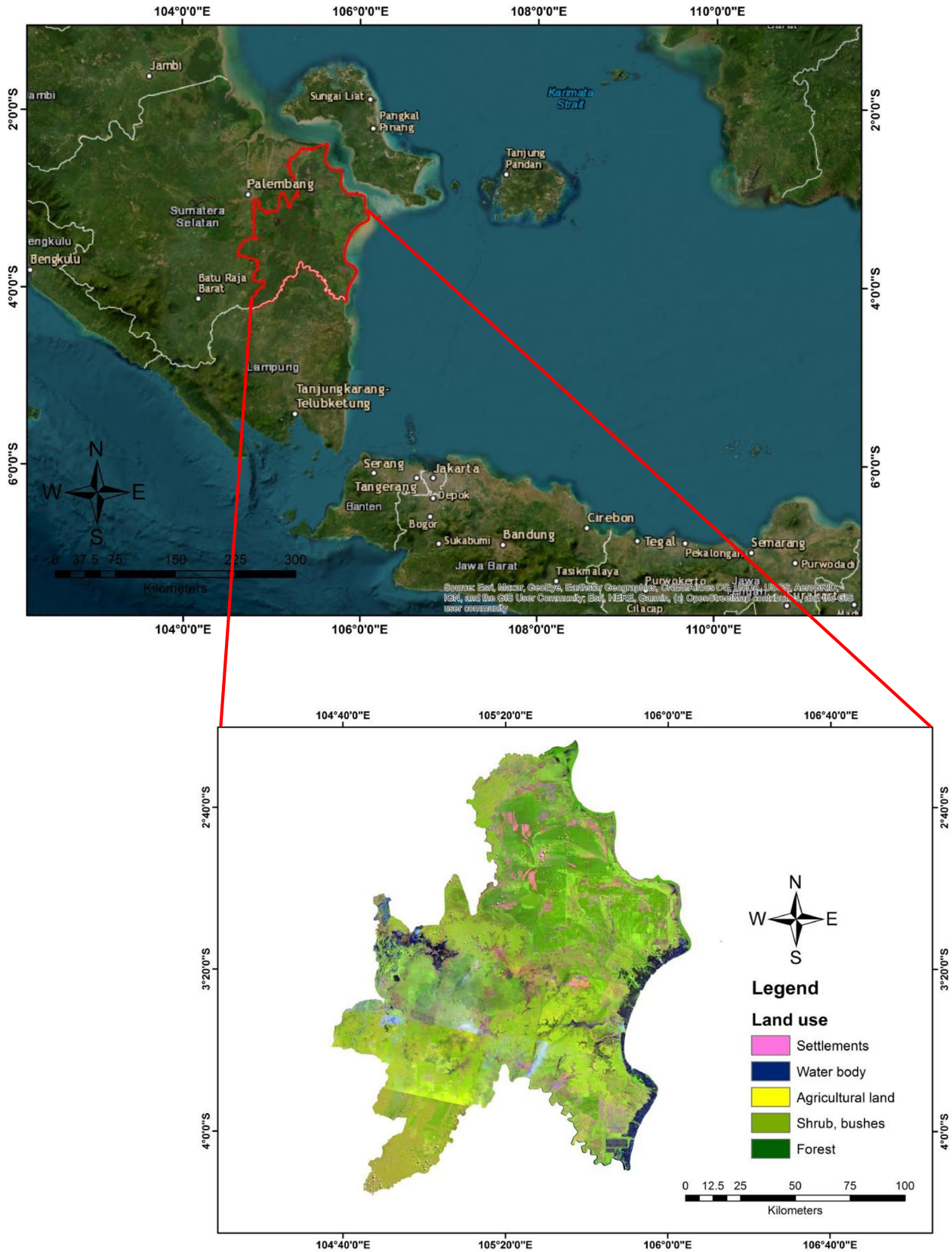


Fig. 1 Location of the study area

in in South Sumatera during 2015 led to the production of smog which disseminate to Malaysia and Singapore regions.

The OKI region has 327 villages and the population of approximately 769,348 people. The OKI's geographical feature is its nearly flat terrain (slope 0–2%) with tropical climate condition. The dry season occurs from April to September, while the wet season occurs from October to March. The annual precipitation in this area ranges between 2,600 and 2,900 mm per year, with a mean temperature of around 31 °C (Fig. 2a). The area's major soil types are humic gravel and organic soil, both of which are associated with water.

One of the unique features that affect the physical condition of the OKI is the area that is mostly covered with wetland. Around 639,122 ha of the OKI were encompassed by peatland, which is equivalent to 50.6% of the peatland in all of South Sumatra province [26]. If we compared the forest fire area of Indonesian provinces in 2019, the South Sumatra showed the highest forest fire area ($3.28 \times 1000 \text{ km}^2$), followed by Central Kalimantan ($3.04 \times 1000 \text{ km}^2$), West Kalimantan ($1.51 \times 1000 \text{ km}^2$), and East Nusa Tenggara ($1.36 \times 1000 \text{ km}^2$) [27]. Peat fires are very flammable, they can cause localized fires to disperse and resulting them hard to cease. Peat catches fire easily and hard to estimate when they begin from the underground. The fires can infiltrate to the soil and spread underground that are difficult for fire fighter to extinguish the fire. The land cover of the study area consisted of areas with forest, shrub, agricultural land like oil palm and rubber, and settlements. The land cover becomes one of important indicators for fire events because the areas like forests and agricultural lands often found fire cases in the OKI region. The human activities which convert the forest into agricultural and settlements have led to severe land fires in the study area every year.

As a result of this situation, the OKI has become the leading cause of land fires in the province of South Sumatra. The OKI was responsible for approximately 51% of the total burned areas in the South Sumatra province in 2015 [28]. According to the authority, total hotspots in 2015 and 2019 were 17,532 and 4,583, respectively. In 2021, about 70 ha of land in the OKI were burned again. This area constantly experiences land fire every year, which makes villages within the OKI area fire-prone.

2.2 Data sources

The details of data used in this study as shown in Table 1. In order to analyze the impact of drought severity, land use, and surface temperature changes in the OKI area, we used the Landsat 8 satellite images to generate the normalized difference moisture index (NDMI), the normalized

difference vegetation index (NDVI), and the land surface temperature index (LST). The details procedure about these above-indexes would be explained in the following section. The Landsat 8 was chosen in this study because of its temporal and spatial resolution, which are appropriate for land fire risk studies. The use of the NDMI index using SWIR band causes Landsat 8 OLI/TIRS more chosen than other satellite images without SWIR band. Furthermore, Landsat 8 satellite can acquire more than 1,000 scenes daily. They are available for download in six hours of acquisition. Thus, Landsat 8 is very suitable for monitoring forest fires.

To improve the accuracy of fire risk analysis, our study investigated the fire pattern across a year. We obtained the highest number of land fire occurrences and burned areas occurred during a dry season, especially in July, August, and September 2021. Therefore, we averaged each of NDMI, NDVI, LST, and SPI variables according the three months. For hotspots data, we collected from the Indonesain Ministry of Environment and Forestry from July to September 2021 which they are originally extracted from NASA-MODIS, NASA-SNPP, and NASA-NOAA20 satellites. The data should have high realibility because it is organized by the government. The accuracy of satellite data is directly checked by the field team and they regularly report to the center office. Annual precipitation data for the current period (2021 year) were obtained from the meteorological stations distributed throughout the study area (<https://www.bmkg.go.id/>). While, for projected future fire risk period (2021–2040 and 2041–2060), we used same variables to generate the future land fire risk map such as NDMI, NDVI, LST, and SPI maps. But, for this future fire risk analysis, we used the future LST and SPI data which corresponding to future periods; 2021–2040 and 2041–2060. The data could be obtained from the WorldClim website.

2.3 Preparation of associated-variables for land fire risk

2.3.1 NDMI analysis

The NDMI calculation algorithm is similar to other vegetation indexes calculated in ArcGIS software using the raster calculator. The surface temperature usually increases because of the shortage of water for evaporation during drought conditions. The NDMI is a specific index that is applied together with LST and NDVI to analyze soil moisture content. The NDMI evaluates the soil moisture content for all features on the earth's surface, so it makes a good benchmark for drought. The NDMI has a range of values greater than 0.1 representing high humidity and less than 0 representing low

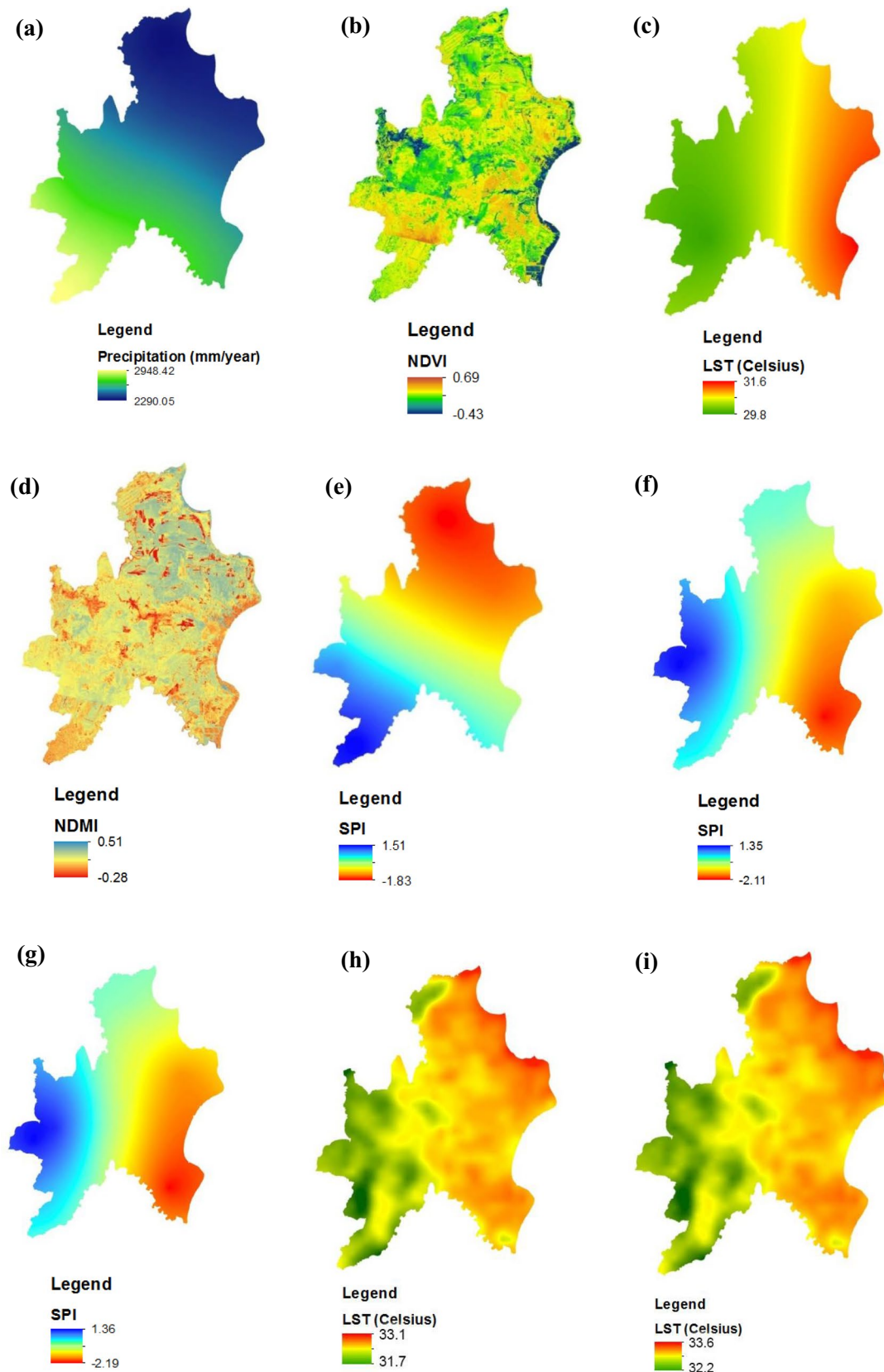


Fig. 2 Environmental variables used for fire risk model, **a** precipitation, **b** NDVI, **c** LST in 2021, **d** NDMI, **e** SPI in 2021, **f** SPI during 2021–2040, **g** SPI during 2041–2060, **h** LST during 2021–2040, and **i** LST during 2041–2060

Table 1 Details of data used in this study

Data	Sources
Landsat 8 OLI/TIRS	USGS Earth Explorer
Boundary of the study area	https://tanahair.indonesia.go.id/
Hotspots data	https://sipongi.menlhk.go.id/
Current precipitation (in 2021)	Meteorological, Climatological, and Geophysical Agency
Predicted precipitation, temperature (2021–2040, 2041–2060)	https://www.worldclim.org/

Table 2 The NDMI classification for this study

NDMI values	Interpretation
– 1–0	High water stress
0–0.2	Moderate water stress
0.2–0.4	Low water stress
> 0.4	Very low water stress, no water stress

Table 3 The NDVI classification for this study

NDVI values	Interpretation
< 0	Water body
0–0.2	Dry
0.2–0.4	Moderate
> 0.4	Wet

Modified from: Aziz et al. [48]

humidity (Table 2). The NDMI raster map is calculated from Landsat 8's SWIR (band 6) and NIR (band 5) wavelengths (Jin and Sader, 2005), as shown in Eq. 1.

$$\text{NDMI} = (\text{NIR} - \text{SWIR}) / (\text{NIR} + \text{SWIR}) \quad (1)$$

2.3.2 NDVI analysis

The NDVI is widely applied in vegetation cover monitoring. This index is appropriate for estimating the vegetation frequency, which is measured at near infrared and red wavelengths. Recently, the NDVI is not only able to analyze the density and health of vegetation, but it can also determine the drought level (Table 3) in distinct areas of the world [29]. The NDVI raster map was produced using the calculation of Landsat 8 bands (band 5 for NIR and band 4 for red), as shown in Eq. 2 below [30].

$$\text{NDVI} = (\text{NIR} - \text{RED}) / (\text{NIR} + \text{RED}) \quad (2)$$

Table 4 The SPI classification for this study

SPI values	Interpretation
– 2–1.5	Severe drought
– 1.5–1	Moderate drought
– 1–0	Slight drought
0–1	Relatively wet
1–2	Very wet

Modified from: Rabiei et al. [15]

2.3.3 LST analysis

Recent advances in remote sensing technology have enabled the determination of land surface temperature (LST) raster maps using a thermal band of satellites. Although the LST may be analyzed using several satellites, in this study we used band 10 of Landsat 8 images to assess it. The LST equation is shown as specified below using a common formula derived from the United States Geological Survey (USGS).

$$\text{LST} = \left(\frac{BT}{1 + 1(W \times \frac{BT}{\rho} \times \ln(e))} \right) - 273.15 \quad (3)$$

where BT is at sensor brightness temperature, W is the radiated radiance wavelength, e is emissivity, and ρ is 1.438×10^{-2} m K.

2.3.4 SPI analysis

The standard precipitation index (SPI) is a specific index that measures the likelihood of precipitation in a certain period so that the user can determine the drought severity. In this study, we used annual precipitation from the current period in 2021 to calculate the SPI value during that year. Meanwhile, for future periods, this study used the mean rainfall derived from the CMIP6. In the CMIP6, we chose a GCM type of HadGEM3-GC31-LL and SSPs 126 for the time study periods: 2021–2040 and 2041–2060. Several studies have revealed that the HadGEM3-GC31-LL showed satisfactory result [31, 32]. The calculation of the SPI value was carried out per grid cell in GIS software. The drought severity classification according to SPI value is tabulated in Table 4. The SPI value can be obtained from Eq. 4 below [33].

$$\text{SPI} = \frac{P_i - P}{S} \quad (4)$$

where P_i is the total amount of rainfall in the studied period, P is the long-range mean of rainfall in the studied period, and S is the standard deviation of rainfall values.

The SPI values from meteorological stations and their respective coordinates were inputted in ArcGIS. A Kriging interpolation technique was conducted to produce an SPI raster map in the study area.

2.4 Current and future land fire risk analysis

The current land fire risk map was produced by overlaying the NDMI, NDVI, LST_{2021} , and SPI_{2021} maps. This process was conducted using the weighted overlay tool in ArcGIS software. The default setting of equal influence was applied for this analysis. Then, using 30 ground hotspot points of data, the current land fire risk map was validated. The validation was carried out using percentages of points in each fire risk category in Microsoft Excel. Meanwhile, the projected future land fire risk map was produced by overlaying the NDMI, NDVI, $LST_{2021-2040}$, $SPI_{2021-2040}$, $LST_{2041-2060}$, and $SPI_{2041-2060}$ map.

3 Results and discussion

3.1 The associated environmental variables for land fire risk

In this study, we applied the NDVI as one of the most popular methods to be used because it was reliable and simply to compute index with only two spectral bands. Based on the NDVI map in Fig. 2b, the NDVI value of the study area increased from southwest to southeast in 2021. The southeast areas consisted of low vegetation cover and toward southeast showed an increase to dense vegetation cover area. The NDVI value varied from -0.43 to 0.69 during the study period. Our result was in line to a study by Rutkay et al. [34] which found the area that exposed by fire showed the NDVI value ranged from 0.1 to 0.3. Our result also obtained the area with the high fire risk had the NDVI value was less than 0.2. A study by Nath and Nath [35] found the average NDVI value after a week of fire event showed the alteration of greenness. Thus, we assumed the fire event has resulted to the change of greenness of the burned vegetations and then reduced their NDVI value. The correlation analysis showed 75% of NDVI map associated with fire risk map (Table 5). This result was consistent with another study by Lasaponara et al. [36] in Italian peninsula also obtained more than 80% accuracy value.

The assessment of LST is one of the rapid methods for fire risk studies. Therefore, many studies have stated the

LST to be the most prominent factors for fire risk [37]. The LST map of the study area showed the high temperature zones from the northwest to the southwest. The LST value varied from 29.8 to 31.6 °C during the current study period (Fig. 2c). It was much lower than a study in Jharkhand forest of India which obtained the LST ranging from 29.4 to 49.5 °C. There were several factors that affected the LST change in a certain area. In the case of the Jharkhand forest of India, the hotspots were found in this study around 198 with 130.3 km² burnt areas. Therefore, forest fire events were particularly more dominant in that area as compared with our study. A previous study by Burdun et al. [38] have reported the LST exhibited the high relationship with in situ observation in the peatland area. A similar result was also reported by Yang [39], where they found the increase in 1.5 °C of LST might increase fire events.

The NDMI is one of indicators that used for fire studies which it was useful to assess the level of moisture stress in vegetation. The NDMI was found more effective as compared with the NDVI in evaluating the moisture content of vegetation. In this study, the NDMI map has been generated using the calculation of NIR and SWIR bands. The NDMI value ranged from -0.28 to 0.51 where the high value indicated the low water stress condition, while low values were the high water stress condition (Fig. 2d). Our result obtained the negative value of NDMI which based on another study by Hao et al. [40], it was attributed from the fire effect that absorbs much water in vegetation. This condition would increase the intensity of forest fire. Contrarily, other areas with low fire risk showed the positive NDMI. These areas were indicated with color green and showed the low fire occurrences. A study of forest fire in Iran revealed the NDMI value ranging from -0.21 to 0.60 [41]. This result was not much different with our study. It showed that there was not a substantial difference of the characteristic forest fire at both areas. In addition, the correlation analysis showed the strong relationship between NDMI and the predicted fire risk map with the value of 86% (Table 5). Rabiei et al. [15] also reported the high association between NDMI and fire risk occasions in the forest of Golestan province. In this study, we also evaluated the SPI index to examine the impact of precipitation on fire risk. Based on the accuracy analysis, the SPI associated with fire risk with the lowest accuracy at 70% as compared with other variables (Table 5). This result was in line to another study by Vlassova et al. [42] which also showed the weak association.

3.2 Current and projected land fire risk maps

According to the current land fire risk map of the study area, high fire risk areas were identified in the northern

Table 5 Comparison of percentage correlation values between the studied variable with fire risk zone map using baseline data in 2021

NDMI	NDVI	LST	SPI
0.86	0.75	0.72	0.70
86%	75%	72%	70%

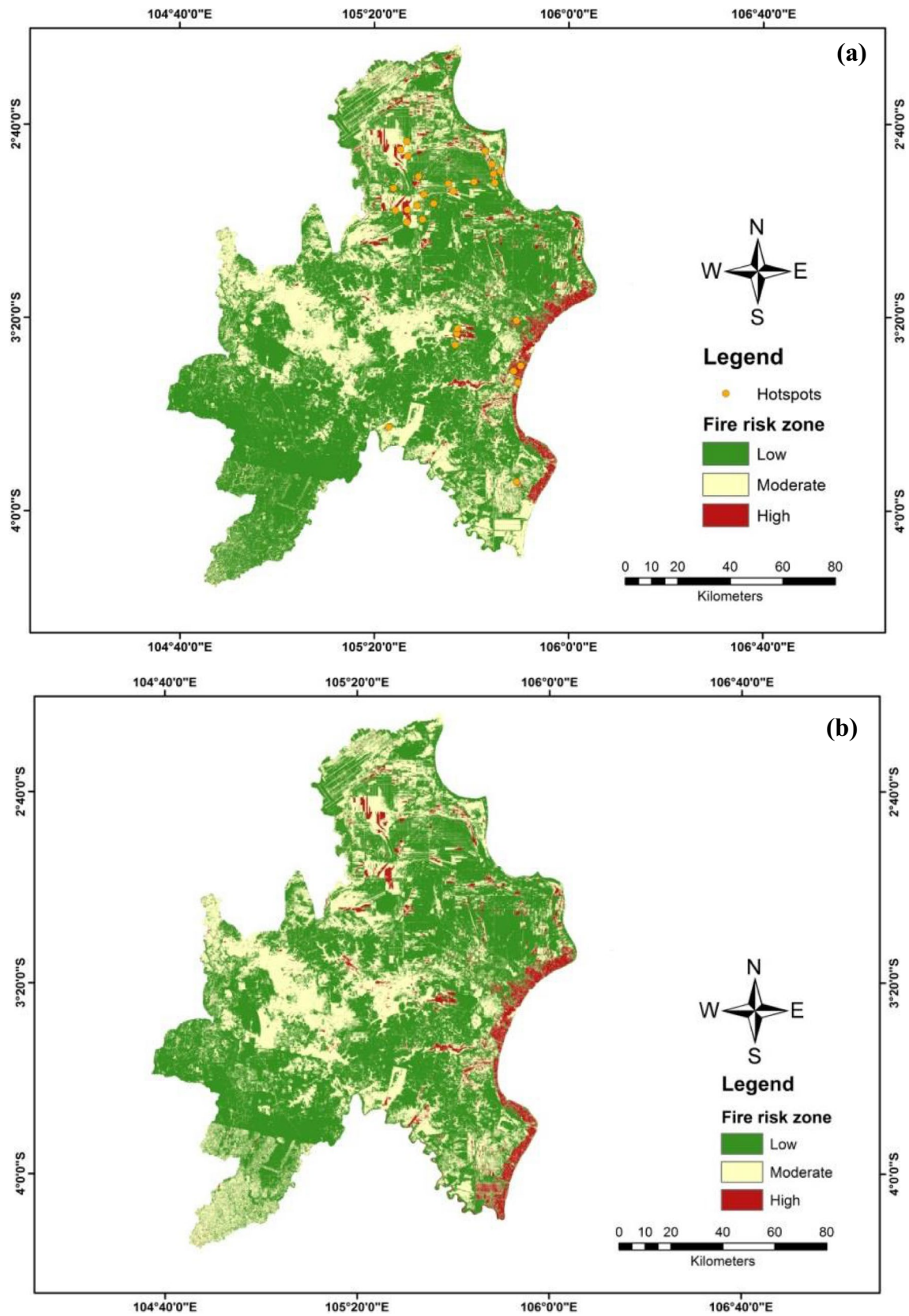


Fig. 3 The projected future fire risk map of the study area, **a** current period of 2021, **b** period of 2021–2040, and **c** period of 2041–2060

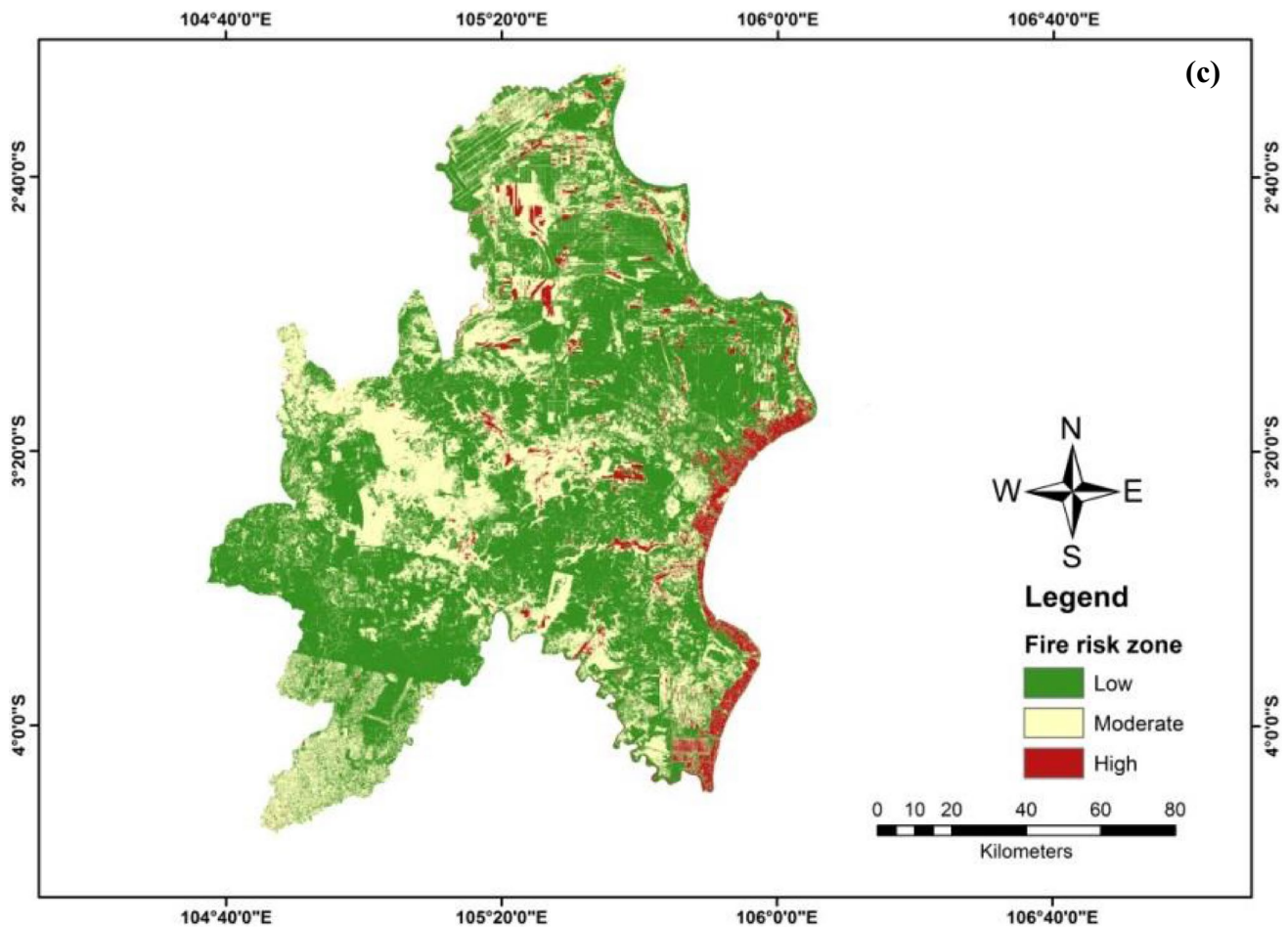


Fig. 3 (continued)

and southeastern region of the study area (Fig. 3a). Details of percentage of fire risk class area were shown in Table 7. The high fire risk class had a total area of 726.4 km² or around 4.2% of the whole study area. Dominant of the class area was under agricultural land. We considered this class was critical because it had the highest susceptibility on fire which was showed by the lowest NDMI and NDVI values. If we compared to another study, we found the high fire risk area in our study was lower than a study of the Parambikulam Tiger Reserve, Kerala, India that obtained approximately of 71% of the study area classified into high fire risk class [43]. This difference might be due to the size of the study site that much larger than our study. Furthermore, if we matched the high fire risk class with LST map, we found that most of class located in the high LST value zones. It showed the class consisted of sparse vegetation cover and might sustain fire event in the past period. The land in the study area was categorized as peatland, it clearly increased the susceptibility of fire. This would make the area very hard to extinguish when the land is burning. Moreover, medium fire risk areas were

mostly found in the middle part of the study area, from the eastern to the northern parts. The medium fire risk class covered about 5621.3 km² or 32.7% of the whole study area. The majority of the class area was under sparse vegetation such shrub and bushes. In contrast, around 10,835.3 km² or 63.1% of the study area was at low fire risk class. The class area was under medium to dense forests. Table 6 showed the accuracy analysis between the hotspots data from the government and our predicted fire risk map. The high fire risk class which produced by this study showed

Table 6 The accuracy assessment of fire risk zones in this study using baseline data in 2021

	Fire points	Low risk area	Moderate risk area	High risk area
Number of points	30	2	3	25
Percentage of points	100	6.6%	10%	83.3%

Table 7 Percentage area of fire risk classes in the study area

Fire risk class	Periods					
	2021		2021–2040		2041–2060	
	Area (km ²)	Area (%)	Area (km ²)	Area (%)	Area (km ²)	Area (%)
Low	10835.3	63.1	10140.5	59.0	10140.5	59.0
Moderate	5621.3	32.7	6212.8	36.2	6098.4	35.5
High	726.4	4.2	829.6	4.8	944.1	5.5

the highest perfect match with the hotspot data from the government by 83.3%.

As we knew, the human activities were the main contributor on the climate change phenomenon. Thus, our climate was not stable anymore. The climate change has significantly affected the quality of soil, air, and water. According to the authority report for 2019, there were about 353 hotspots in the South Sumatra region, which were recorded as the worst fire cases for this decade. Our study estimated that the drought level in the future period would become worse than the current period. It was shown by the discrepancy between SPI maps of the current and future periods (Figs. 2e–g). The SPI value decreased from -1.85 to -2.11. A regional study by Alfahmi et al. [44] in Sumatera, Indonesia also obtained the negative SPI value which it related to the increasing total of hotspots. Also, there was a notable increase in future LST value with 6% increment as compared with the current period (Figs. 2h–i). This result was consistent with another study in Iraq which forecasted the LST raised from 38 to 40.8 °C in the future [45]. As a result of this circumstance, our study found a significant increase of total high fire risk area from 726.4 km² to 829.6 km² during 2021–2040. Then, it continued to rise from 829.6 km² to 944.1 km² during 2041–2060 (Table 7). The projected fire risk map of the study area was shown in Figs. 3b–c. But, the predicted result was only considered if the land use status of the study area did not change or changed slightly, as mentioned in a study by Cochrane and Laurance [46]. Because the study area was categorized as rural area, we assumed the land use conversion was slower.

For moderate fire risk areas sustained an increase during 2021–2040, but it slightly reduced during 2041–2060. This might be due to the conversion of the area from moderate to high class. On the other hand, the total of low fire risk area decreased from 10,835.3 km² to 10,140.5 km² during 2021–2040 and remained constant during 2041–2060. This reduction obviously increased the chance of land fire occasions in the study area. Our study had a limitation since we could not include the land cover change for the projected future fire risk analysis. The analysis of future fire risk in the study area might be impacted by ongoing

deforestation and land cover conversion. The land cover conversion would affect the projected fire risk analysis, for instance the increment of agricultural lands would increase the fires due to the burning biomass, opening new lands, and replanting activities [47]. Thus, the potential increase in fire risk areas was an arduous challenge for the authority to arrange an effective policy to mitigate land fire issues in the OKI region.

4 Conclusions

Our study concluded the study area sustained the higher risk of fire events in the future periods; 2021–2040 and 2041–2060 as compared with the current period in 2021. The fire risk areas were found to be more concentrated in the eastern part of the study area, and it would expand to the southern part according to our projected fire risk map. The high fire risk areas were indicated as the low NDMI values. We highlighted that the land cover conversion affected the projected fire risk analysis. The increasing of agricultural areas would increase fires due to the burning biomass, opening new lands, and replanting activities. Therefore, these findings will be beneficial for authorities to provide the necessary actions to prevent fires events in the study area.

Author contributions Conceptualization and supervision: MR; writing review and editing: MR, WMRI, SAR, and HGA; data curation and formal analysis: MR, WMRI, and SAR; evidence collection, review, and editing: HGA, HA, AAAD, and JAA.

Funding Not applicable.

Data and material availability The datasets used and/or analyzed during the current study are available from the corresponding author on reasonable request.

Declarations

Conflict of interest The authors have no relevant financial or non-financial interests to disclose.

Ethics approval and consent to participate Not applicable.

Consent for publication Not applicable.

Open Access This article is licensed under a Creative Commons Attribution 4.0 International License, which permits use, sharing, adaptation, distribution and reproduction in any medium or format, as long as you give appropriate credit to the original author(s) and the source, provide a link to the Creative Commons licence, and indicate if changes were made. The images or other third party material in this article are included in the article's Creative Commons licence, unless indicated otherwise in a credit line to the material. If material is not included in the article's Creative Commons licence and your intended use is not permitted by statutory regulation or exceeds the permitted use, you will need to obtain permission directly from the copyright holder. To view a copy of this licence, visit <http://creativecommons.org/licenses/by/4.0/>.

References

- Führer E (2000) Forest functions, ecosystem stability and management. *Forest Ecol Manag* 132(1):29–38. [https://doi.org/10.1016/S0378-1127\(00\)00377-7](https://doi.org/10.1016/S0378-1127(00)00377-7)
- Abdo HG, Almohamad H, Al Dughairi AA, Al-Mutiry M (2022) GIS-based frequency ratio and analytic hierarchy process for forest fire susceptibility mapping in the western region of Syria. *Sustainability* 14(8):4668. <https://doi.org/10.3390/su14084668>
- Attri V, Dhiman R, Sarvade S (2020) A review on status, implications and recent trends of forest fire management. *Arch Agri Env Sci* 5(4):592–602. <https://doi.org/10.26832/24566632.2020.0504024>
- Driscoll DA, Armenteras D, Bennett AF et al (2021) How fire interacts with habitat loss and fragmentation. *Biol Rev* 96(3):976–998. <https://doi.org/10.1111/brv.12687>
- Rendana M, Idris WMR, Abd Rahim S (2022) Effect of COVID-19 movement control order policy on water quality changes in Sungai Langat, Selangor, Malaysia within distinct land use areas. *Sains Malays* 51:1587–1598. <https://doi.org/10.17576/jsm-2022-5105-26>
- Alauddin M, Hossain M, Islam M et al (2020) Management strategies for sustainable forest biodiversity conservation in protected areas of Bangladesh: a study of Bhawal national park. *Gazipur Grassroots J Nat Resour* 3(3):56–72. <https://doi.org/10.2139/ssrn.3874824>
- Chandra N, Singh G, Rai ID, Mishra AP, Kazmi MY, Pandey A, Abdo HG (2023) Predicting distribution and range dynamics of three threatened cypripedium Species under climate change scenario in Western Himalaya. *Forests* 14(3):633. <https://doi.org/10.3390/f14030633>
- Rendana M, Idris WMR, Rahim SA (2021) Atmospheric methane condition over the south sumatera peatland during the COVID-19 pandemic. *Aerosol and Air Qual Res* 21(10):210072. <https://doi.org/10.4209/aaqr.210072>
- Firmansyah MF, Rusliana N, Johar S et al (2022) The influence of ASEAN agreement on transboundary haze pollution for emission changes in Indonesia. *Indonesian J Soc and Env Issues* 3(1):89–100. <https://doi.org/10.47540/ijsei.v3i1.374>
- Minardi A, Taufik T, Astuti D et al (2020) Singapore country assistance to help extinguish forest fire in South Sumatera. *Sriwijaya J Env* 5(1):53–59. <https://doi.org/10.22135/sje.2020.5.1.53-59>
- Abedi Gheshlaghi H, Feizizadeh B, Blaschke T (2020) GIS-based forest fire risk mapping using the analytical network process and fuzzy logic. *J Environ Plan Manag* 63(3):481–499. <https://doi.org/10.1080/09640568.2019.1594726>
- Ghorbanzadeh O, Blaschke T, Gholamnia K et al (2019) Forest fire susceptibility and risk mapping using social/infrastructural vulnerability and environmental variables. *Fire* 2(3):50. <https://doi.org/10.3390/fire2030050>
- Ozenen Kavlak M, Cabuk SN, Cetin M (2021) Development of forest fire risk map using geographical information systems and remote sensing capabilities: ören case. *Env Sci Pol Res* 28(25):33265–33291. <https://doi.org/10.1007/s11356-021-13080-9>
- Thomas Ambadan J, Oja M, Gedalof ZE et al (2020) Satellite-observed soil moisture as an indicator of wildfire risk. *Rem Sens* 12(10):1543. <https://doi.org/10.3390/rs12101543>
- Rabiei J, Khademi MS, Bagherpour S (2022) Investigation of fire risk zones using heat–humidity time series data and vegetation. *Appl Water Sci* 12(9):1–12. <https://doi.org/10.1007/s13201-022-01742-z>
- Sakellariou S, Cabral P, Caetano M et al (2020) Remotely sensed data fusion for spatiotemporal geostatistical analysis of forest fire hazard. *Sensors* 20(17):5014. <https://doi.org/10.3390/s20175014>
- Liu Z, Ballantyne AP, Cooper LA (2019) Biophysical feedback of global forest fires on surface temperature. *Nat Commun* 10(1):1–9. <https://doi.org/10.1038/s41467-018-08237-z>
- Glushkov I, Zhuravleva I, McCarty JL et al (2021) Spring fires in Russia: results from participatory burned area mapping with sentinel-2 imagery. *Environ Res Lett* 16(12):125005. <https://doi.org/10.1088/1748-9326/ac3287>
- Achour H, Toujani A, Trabelsi H et al (2021) Evaluation and comparison of Sentinel-2 MSI, Landsat 8 OLI, and EFFIS data for forest fires mapping. Illustrations from the summer 2017 fires in Tunisia. *Geocarto Int* 1–20. <https://doi.org/10.1080/10106049.2021.1980118>
- Shi C, Liang Y, Gao C et al (2020) Drought-modulated boreal forest fire occurrence and linkage with La Nina events in Altai Mountains. *Northwest China Atm* 11(9):956. <https://doi.org/10.3390/atmos11090956>
- Berenguer E, Lennox GD, Ferreira J et al (2021) Tracking the impacts of El niño drought and fire in human-modified Amazonian forests. *Proc Natl Acad Sci* 118(30):e2019377118. <https://doi.org/10.1073/pnas.2019377118>
- Wang G, Cai W (2020) Two-year consecutive concurrences of positive Indian ocean dipole and central pacific El Niño preconditioned the 2019/2020 Australian “black summer” bushfires. *Geosci Lett* 7(1):1–9. <https://doi.org/10.1186/s40562-020-00168-2>
- Liu G, Li J, Ying T et al (2023) Atlantic multi-decadal oscillation modulates the relationship between El Niño–Southern Oscillation and fire weather in Australia. *Atmos Chem Phys Discuss* 2023:1–17. <https://doi.org/10.5194/acp-2022-858>
- Nurdiati S, Bukhari F, Julianto MT et al (2022) The impact of El Niño southern oscillation and Indian ocean dipole on the burned area in Indonesia. *Terr Atmospheric Ocean Sci* 33(1):16. <https://doi.org/10.1007/s44195-022-00016-0>
- Purwandani A, Ardiyanto R, Sumargana L et al (2019) Is Land and Forest Fire in Ogan Komering Ilir, Southern Sumatera, Affected by Climate Change?. In: IEEE Asia-Pacific Conference on Geoscience, Electronics and Remote Sensing Technology pp. 95–98. IEEE. <https://doi.org/10.1109/AGER548446.2019.9034289>
- Hadiyani FS, Nurhayati AD (2022) Hotspot analysis in 2015 and 2019 at ogan komering ilir district south Sumatera province. *IOP Conf Series Earth and Environ Sci* 959(1):012056. <https://doi.org/10.1088/1755-1315/959/1/012056>
- Andarini DF, Cholianawati N, Indrawati A (2021) Forest fire in east nusa tenggara during 2015–2019: comparison to forest fire in Kalimantan and Sumatera. *IOP Conf Series: Earth and Environ*

- Sci 893(1):012010. <https://doi.org/10.1088/1755-1315/893/1/012010>
28. Kushartati B (2017) implementasi kebijakan pengendalian kebakaran hutan dan lahan di provinsi sumatera selatan. *J Anal Kebijak Kehutan* 14(2):165–186. <https://doi.org/10.36982/jam.v1i2.338>
29. Sruthi S, Aslam MM (2015) Agricultural drought analysis using the NDVI and land surface temperature data; a case study of Raichur district. *Aquat Procedia* 4:1258–1264. <https://doi.org/10.1016/j.aqpro.2015.02.164>
30. Rouse JJW, Haas RH, Schell JA et al. (1973) Monitoring the vernal advancement and retrogradation (green wave effect) of natural vegetation (No. NASA-CR-132982).
31. Abbas A, Ullah S, Ullah W et al (2022) Evaluation and projection of precipitation in Pakistan using the coupled model inter-comparison project phase 6 model simulations. *Int J Climatol* 2022:1–8. <https://doi.org/10.1002/joc.7602>
32. Zareian MJ, Dehban H, Gohari A (2022) Evaluation of the accuracy of CMIP6 models in estimating the temperature and precipitation of Iran based on a network analysis. *Water Irrig Manag* 12(4):783–797. <https://doi.org/10.22059/jwim.2022.345975.1006>
33. McKee TB, Doesken NJ, Kleist J (1993) The relationship of drought frequency and duration to time scales. In: *Proceedings of the 8th Conference on Applied Climatology* 17(22): 179–183
34. Rutkay ATUN, Kalkan K, Gürsoy Ö (2020) Determining the forest fire risk with sentinel 2 images. *Turkish J Geosci* 1(1):22–26
35. Nath A, Nath R (2019) Identification of black dragon forest fire in Amur river basin using satellite borne NDVI data and its impact on long range transport of pollutants: a case study. *J Atmos Sci Res* 2(3):6–10. <https://doi.org/10.30564/jasr.v2i3.1182>
36. Lasaponara R, Abate N, Fattore C et al (2022) On the use of sentinel-2 NDVI time series and google earth engine to detect land-use/land-cover changes in fire-affected areas. *Rem Sens* 14(19):4723. <https://doi.org/10.3390/rs14194723>
37. Çolak E, Sunar F (2020) Evaluation of forest fire risk in the mediterranean turkish forests: a case study of Menderes region, Izmir. *Int J Disaster Risk Reduct* 45:101479. <https://doi.org/10.1016/j.ijdrr.2020.101479>
38. Burdun I, Kull A, Maddison M et al (2021) Remotely sensed land surface temperature can be used to estimate ecosystem respiration in intact and disturbed northern peatlands. *J Geophys Res Biogeosci* 126(11):e2021JG06411
39. Yang S (2021) The relationship between land surface temperature anomalies and fire occurrence in Cariboo Region in 2017. <https://doi.org/10.14288/1.0396751>
40. Hao B, Xu X, Wu F et al (2022) Long-term effects of fire severity and climatic factors on post-forest-fire vegetation recovery. *Forests* 13(6):883. <https://doi.org/10.3390/f13060883>
41. Kalantar B, Ueda N, Idrees MO et al (2020) Forest fire susceptibility prediction based on machine learning models with resampling algorithms on remote sensing data. *Rem Sens* 12(22):3682. <https://doi.org/10.3390/rs12223682>
42. Vlassova L, Pérez-Cabello F, Mimbbrero MR et al (2014) Analysis of the relationship between land surface temperature and wildfire severity in a series of landsat images. *Rem Sens* 6(7):6136–6162. <https://doi.org/10.3390/rs6076136>
43. Nikhil S, Danumah JH, Saha S et al (2021) Application of GIS and AHP method in forest fire risk zone mapping: a study of the Parambikulam tiger reserve, Kerala, India. *J Geovis Spat Anal* 5(1):14. <https://doi.org/10.1007/s41651-021-00082-x>
44. Alfahmi F, Khaerima A, Byantoro AW (2021) Utilization of ECMWF seasonal rainfall forecast system (SEASS) for forest fire prediction over Sumatera Island, Indonesia. *IOP Conf Series Earth Environ Sci* 893(1):012042. <https://doi.org/10.1088/1755-1315/893/1/012042>
45. Al-Hameedi WMM, Chen J, Faichia C et al (2022) Geospatial analysis of land use/cover change and land surface temperature for landscape risk pattern change evaluation of Baghdad City, Iraq, Using CA–Markov and ANN Models. *Sustainability* 14(14):8568. <https://doi.org/10.3390/su14148568>
46. Cochrane MA, Laurance WF (2008) Synergisms among fire, land use, and climate change in the Amazon. *AMBIO A J Hum Environ* 37(7):522–527. <https://doi.org/10.1579/0044-7447-37.7.522>
47. Rendana M, Idris WMR, Rahim SA et al (2019) Effects of organic amendment on soil organic carbon in treated soft clay in paddy cultivation area. *Sains Malays* 48(1):61–68. <https://doi.org/10.17576/jsm-2019-4801-07>
48. Aziz A, Umar M, Mansha M et al (2018) Assessment of drought conditions using HJ-1A/1B data: a case study of Potohar region. *Pakistan Geomat Nat Haz Risk* 9(1):1019–1036. <https://doi.org/10.1080/19475705.2018.1499558>

Publisher's Note Springer Nature remains neutral with regard to jurisdictional claims in published maps and institutional affiliations.